Journal of Visualization, Vol. 12, No. 2 (2009) 119-130

Regular Paper

Measurement of Airflow of Air-Conditioning in a Car with PIV

Yang, J.H.*[1], Kato, S.*[2] and Nagano, H.*[3]

*1 School of Architecture, Yeungnam University, 214-1 Dae-dong, Gyeongsan-si, Gyeongsanbuk-do, 712-749, Republic of Korea.
E-mail: yangjh@ynu.ac.kr
*2 Institute of Industrial Science, The University of Tokyo, 4-6-1 Komaba, Meguroku, Tokyo 153-8505, Japan.
*3 Graduate School of Engineering, The University of Tokyo, 4-6-1 Komaba, Meguroku, Tokyo 153-8505, Japan.

Received 6 March 2008
Revised 20 August 2008

Abstract : In the present study, a model experiment is performed in order to clarify the airflow characteristics of a car cabin. In addition, this study provides high precision data for a benchmark test using the CFD (Computational Fluid Dynamics) analysis method. Initially, the study focuses on the ventilation mode that describes the flow field in the car cabin obtained from an experiment with PIV. The car cabin model is made of transparent acrylic resin and measures 1,450 mm × 700 mm × 900 mm, almost half the size of a real car, and was installed in a thermostatic chamber. In the experiment, the cabin model was controlled by an orifice tube and a pressure gauge in order to confirm the airflow rate. The PIV measurement was performed at a total of 18 regions within the section. The analyzed PIV data provides the mean velocity profile, the standard deviation distribution and the turbulence intensity distribution at each region.

Keywords : Ventilation, PIV, Car Cabin, Data for Benchmark Test

1. Introduction

Ensuring a comfortable atmosphere within a car is an important concern for passengers. Creating such a comfortable atmosphere calls for the development of a technique that can accurately predict the atmosphere within the car, and that can also improve the existing air-conditioning system.

Several studies have previously been carried out relating to the atmosphere within automobiles. Batterman et al. (2006) proposed the use of tracer gas techniques to accurately measure the concentrations of volatile organic compounds (VOC) in homes and vehicles, and provided a discussion on the usefulness of these techniques. Dag Aronson et al. (2000) measured airflow velocity in a real car, a Volvo S80, and compared the results with those of CFD results. In their study, PIV was used for the velocity measurements, and has also been used for the experiments in this present study. However, in their study, the turbulent intensity inside the cabin was not investigated. Kataoka et al. (1998, 2001) used a three-dimensional laser flow meter to measure the airflow distribution in a simple car model and carried out a benchmark test for a CFD analysis. On the basis of the test results, they also measured the thermal sensations experienced by the passengers. With each of these studies, the experiments were based on a real car, while the detail shapes used in the studies differed from each other.

In the present study, a standard half-scale car model was created in order to conduct a comprehensive experimental study of the atmosphere within a vehicle. The purpose of this report is to provide data that can be used to examine the accuracy of CFD analysis by means of a high precision experiment using PIV. The experimental data is intended to be shared as a standard model that can be used to assess the atmosphere within cars and for use in CFD benchmark tests in the development of automobile air conditioning. As a result, it should become possible to accurately predict the atmosphere in vehicles using CFD and to design high-quality air-conditioning.

2. Experimental Method

2.1 Outline of Car Model

In the present study, a PIV experiment was carried out using a half-scale car model as shown in Figs. 1 and 2. The model is made of transparent acrylic resin and measures 1,450 mm × 700 mm × 900 mm. The top of the model can be opened and closed so as to permit the manipulation of the experimental devices, etc. from above. Ducts are connected to the model from the front in order to supply air to the interior. The model is symmetrical about the centerline.

Fig. 1. Half-scale car model.

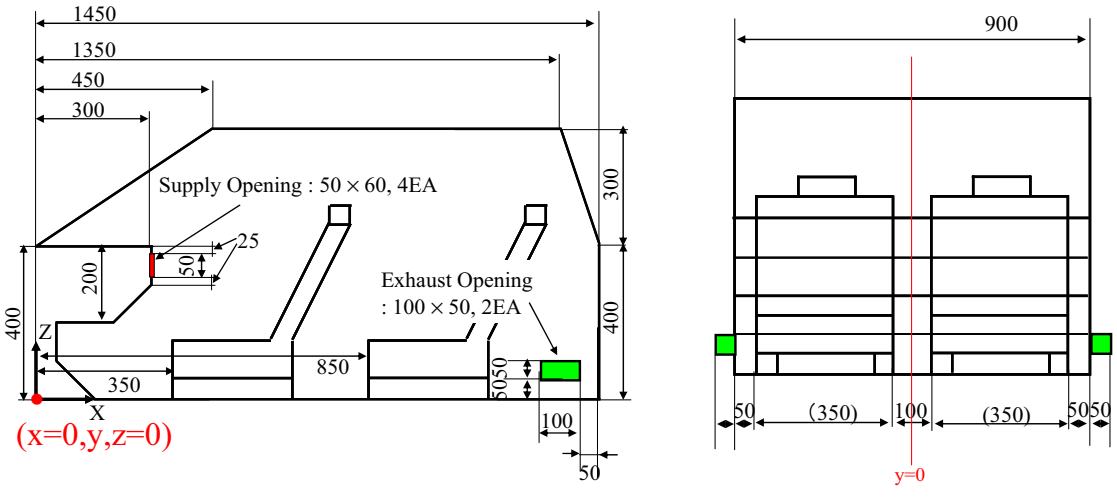

(a) XZ plan (b) YZ plan

Fig. 2. Size of the car cabin model. (unit: mm)

As shown in Figs. 2, 3 and 4, the model is provided with four supply openings in the front for internal air conditioning. A rectangular duct coupled with a flexible duct is connected to each of the supply openings to supply air via a fan. The supply opening dimensions are 50 mm × 60 mm, and the supply angle is 20 degrees. Car air-conditioning can be implemented using various supply angles, and this aspect needs to be reviewed. In the study, the supply angle was set at 20 degrees so that the conditioned air can reach the driver and the passenger in the front seat. This was discussed in the thesis. The air inside the interior of the model is exhausted by fans from two exhaust openings to the rear of the model. The amount of air supplied (exhausted) is controlled to a preset value by adjusting the electric power supplied to the fans. The airflow rate is measured using an orifice tube and the amount of air is regulated with a fan.

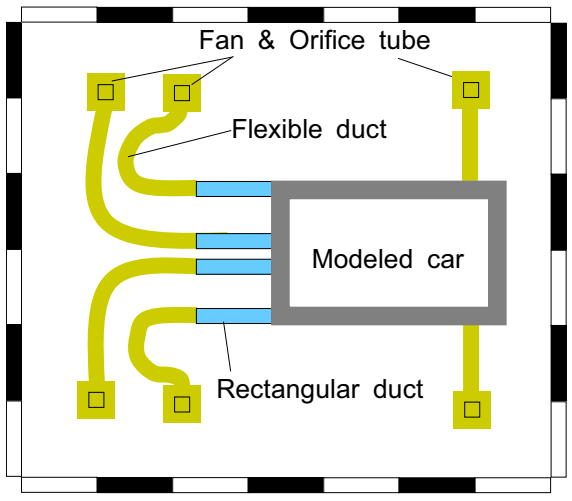

Fig. 3. Floor plan of the climate chamber.

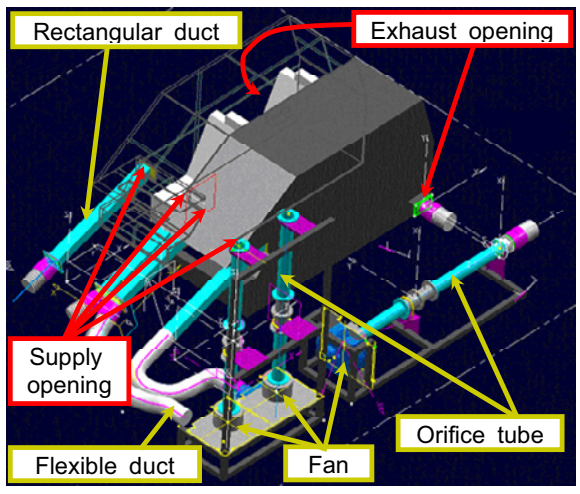

Fig. 4. Experimental equipments set-up.

2.2 Outline of Climate Chamber

The scale model was installed in a thermostatic chamber measuring 3 m × 3.5 m × 2.5 m. This chamber is capable of supplying air from the entire floor and exhausting air from the entire ceiling. The difference in temperature between the top and the bottom can be controlled within 0.1 Kelvin. Once the temperature inside the chamber is constant, the air in the chamber is drawn in by fans and supplied to the interior of the model as air supply for the air conditioning.

2.3 Experimental Equipments Set-up

1) Particle Image Velocimety (PIV)

The PIV system (Dantec PIV-HUB, FlowSense M2 10 bit; NewWave Nd: YAG Laser) as used in the present study is designed to measure two-dimensional airflow velocity distribution. In order to measure airflow velocity using the PIV, tracer particles (oil-based particles 0.25 μm to 60 μm in diameter), which provide ample scattered light, are sprinkled around the fan that is used to air condition the model so that they can first be fed into the model. Images of particles taken at two different times are then input as digital data by a CCD camera that is synchronized with the pulse laser. In each of the inspection regions, the distance traveled by the particles in micro time units is obtained by numerical processes, such as Fourier transformation and correlation, and a velocity vector diagram is calculated.

2) Orifice Tube

The orifice tubes (Fig. 5) that were used in the present experiment were made from transparent acrylic resin in accordance with JIS Z8762-1995. The orifice tube for regulating the airflow rate supplied to the model is 0.06 m in diameter (throttle nozzle diameter: 0.03 m), and the orifice tube for regulating the airflow rate exhausted from the model is 0.06 m in diameter (throttle nozzle diameter: 0.04 m). It is expected that these orifice tubes are capable of accurately measuring the airflow rate (error within approximately 1%), although this depends more or less on the accuracy of the measuring instrument used. In addition, the orifice tube was manufactured to measure 80~300 m^3/h of the airflow. The performance test of the orifice tubes was conducted for flow rates at an air temperature of 300K. Therefore, the temperature inside the thermostatic chamber was also maintained at 300K throughout the experiment.

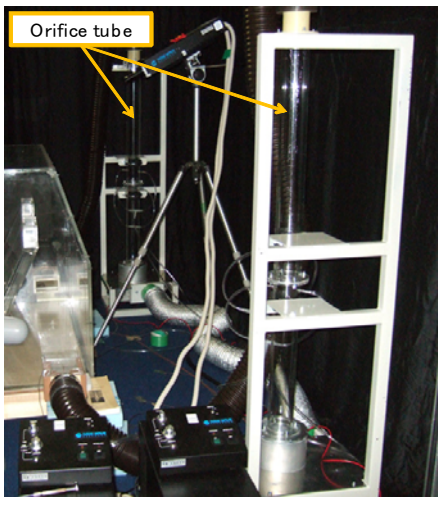

Fig. 5. Outline of orifice tube connected car cabin.

3) Pressure Gauge

In order to measure the airflow rate using an orifice tube, the difference in pressure is initially measured before and after the throttle nozzle of the orifice tube and the airflow rate is then estimated from the relationship obtained from the orifice tube performance test. The BARATRON pressure gauge shown in Fig. 6 is used to measure the difference in pressure before and after the throttle nozzle of the orifice tube. In addition, an NR-2000 made by KEYENCE is used to collect and analyze the electrical signals obtained from the pressure gauges.

Fig. 6. Pressure gauge for control of airflow rate.

3. Deciding on Airflow Rate

The scale model constitutes a closed space. Consequently, when the model interior is air-conditioned, a difference in pressure occurs both inside and outside the model, rendering it difficult to accurately regulate the flow rates of supply air and exhaust air. Therefore, it is necessary to determine the output of each of the fans connected to the orifice tubes so that the preset airflow rate can be maintained without inducing a pressure differential between the interior and exterior of the model.

In the study, the airflow rate was set based on the similarity in terms of the Reynolds number, so that the actual airflow rate can be simulated in a ½-scale model. A conditioned airflow can be set in stages, and if it is assumed that the stage 1 setup is 160 m^3/h, the airflow becomes 80 m^3/h, according to the Reynolds number. However, since it was assumed that the measurable airflow rate in an orifice tube was to be 80~300 m^3/h in the study, if the airflow rate is set at 80 m^3/h in a car model, then the accuracy of the flow control can be reduced. Conversely, if it is set at a high airflow, the speed of the flow is accelerated, rendering it difficult to track particles according to the PIV. Consequently, the conditioned airflow was set at 100 m^3/h for the experiment conducted in this study. Therefore, as the airflow rate required for the air-conditioning of the interior of the model was set at 100 m^3/h, the difference in pressure both inside and outside the model was measured in order to monitor any unwanted air leakage. A highly accurate airflow is required in order to confirm a zero pressure difference between the inside and the outside. This measurement was performed three times using the pressure gauges and NR-2000. During each measurement, sampling was carried out 1,000 times at 1 Hz. Table 1 shows the air flow rate (average of three measurements) for each of the six fans. Each of the fans from Nos. 1 through to 4 supplies air to the model, with the preset airflow rate being 25 m^3/h. Both fan Nos. 5 and 6 exhaust air from the model, with the preset airflow rate being 50 m^3/h.

Table 1. Pressure differential in orifice tube and airflow rate.

Fan No.	Differential pressure [Pa]	Air volume [m^3/h]	Fan No.	Differential pressure [Pa]	Air volume [m^3/h]
No.1	104.8	24.63	No.4	107.7	24.97
No.2	106.6	24.66	No.5	123.6	48.58
No.3	105.7	25.00	No.6	130.5	49.92

The differences in pressure between the inside and outside of the model were 1.9 Pa, 2.5 Pa and 2.1 Pa. On average, the pressure inside the model was 2.17 Pa higher than the pressure outside

the model. While the flow rate of supply air was 99.26 m^3/h, the flow rate of exhaust air was 98.5 m^3/h, or 99.23%. A highly accurate airflow rate (error around 1% against the preset flow rate) could be secured. By controlling the airflow rate, it is deemed possible to achieve a symmetrical airflow about the centerline in the model.

4. Airflow Measurement with PIV

4.1 Measurement Condition

Using the PIV system previously described, the airflow inside the model that was air-conditioned at the preset airflow rate was measured (100 m^3/h). Fig. 7 shows images taken during these measurements. With the scale model installed in the thermostatic chamber, the airflow in each of the test regions was measured by the PIV system. The temperature inside the thermostatic chamber was set at 300K. During the measurement, however, it rose by approximately 1K as the tracer particles for PIV measurement entered the chamber. Each image shot obtained from the CCD camera is composed of 1,600 × 1,186 pixels and is analyzed using 66 × 49 vectors (3,234 vectors). The PIV measurement was conducted at a total of 18 regions within section Y = 394.5 mm (the center of the window-side supply opening near the driver's seat of the model) (see Figs. 8).

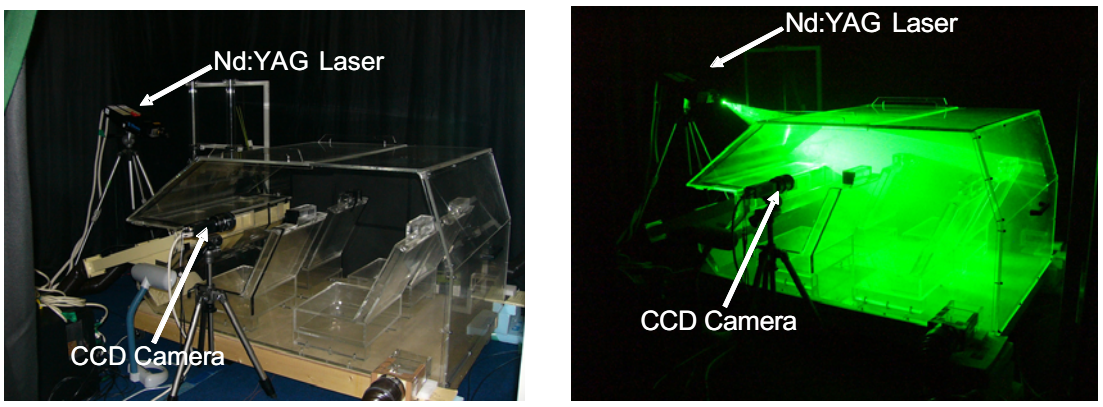

(a) Before measurement (b) During measurement

Fig. 7. Measurement with PIV.

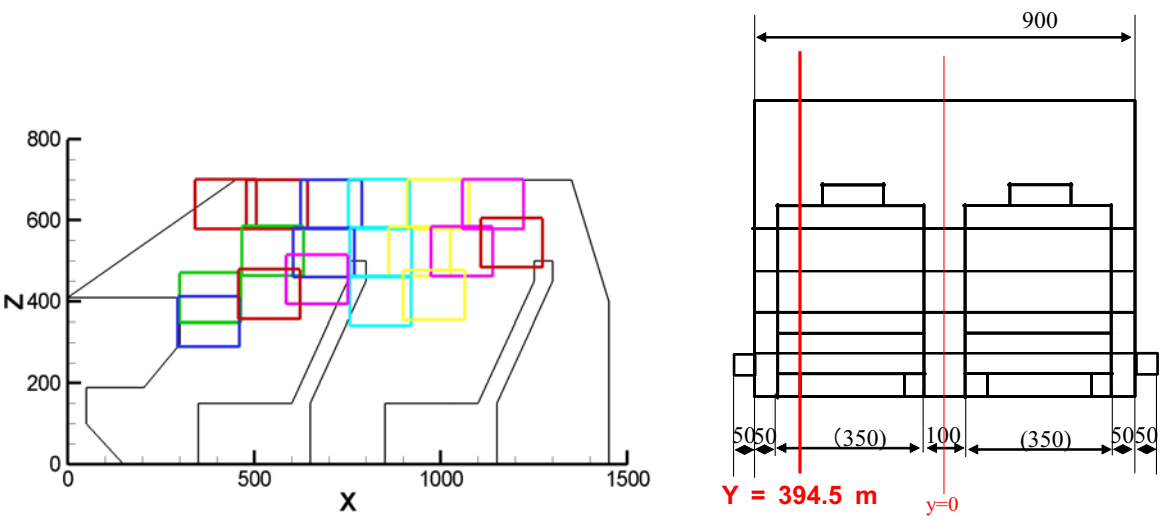

(a) Measurement Region (b) Measurement plan position

Fig. 8. Measurement condition.

4.2 Outline of Analysis

1) PIV Data Analysis

The variable measured using PIV is the instantaneous velocity of a flow field, or two-component velocity information. The instantaneous velocity $\widetilde{u}_i$ is divided into the average velocity component U_i and the velocity variation component u_i, as follows:

$$\widetilde{u}_i = U_i + u_i \tag{1}$$

where, subscript i denotes the velocity component (i = 1, 2). It is necessary to obtain the turbulent flow statistic by calculating the average of the obtained instantaneous velocities. The average velocity can be obtained as an arithmetic mean of the group of instantaneous velocity data as follows:

$$U_i = \frac{\sum_{k=1}^{N} \widetilde{u}_{i,k}}{N} \tag{2}$$

where, N denotes the number of data items used in calculating the average.

In the present experiment, in each of the measurement regions shown in Fig. 8 (a), images were taken at a time separation (200 ~ 1,000 μs depending on the flow velocity measured). 200 sets of such images were taken in each inspection region and were subjected to filtering (adaptive correlation and average filter) to obtain instantaneous velocity data from approximately 200 images. The interrogation area size was set at 32×32, with an overlap at 25% and peak validation at 1.1. The average airflow velocity was then calculated using vector statistics based on Equation 2. As shown in Fig. 9, airflow data in each measurement region was prepared from vector statistics, and the airflow in the model was comprehensively studied using a combination of data collected from 18 regions.

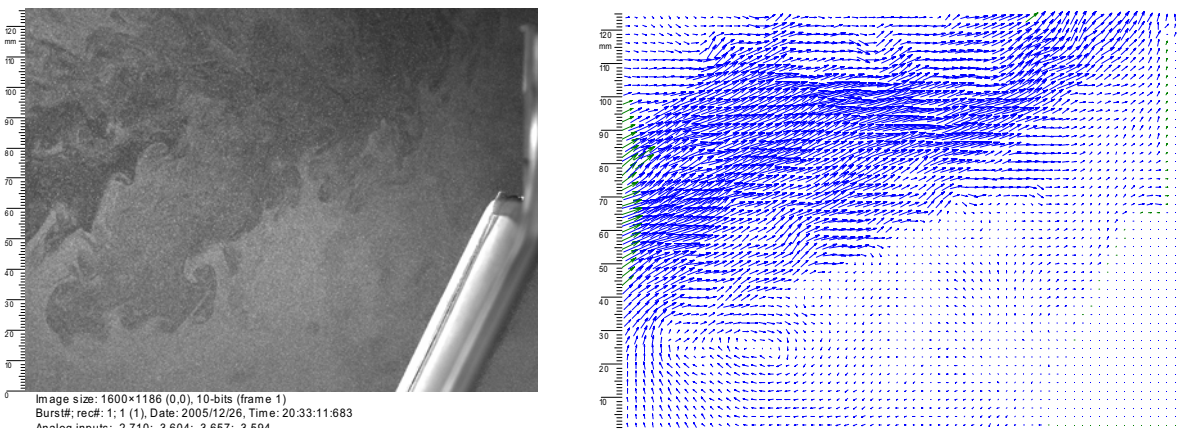

(a) Sample image (b) Vector distribution

Fig. 9. Sample image and result of vector distribution by PIV measurement

2) Mean Velocity Profiles

From each of the four supply openings in the scale model, air was fed into the model at a rate of approximately 25 m^3/h and at an upward angle of 20 degrees in order to air-condition the interior of the model. Under those conditions, 18 points were measured using PIV as measurement regions in the central section of the window-side supply opening near the driver's seat. This was carried out in order to calculate the two-dimensional (UW) average scalar airflow velocity and the average vector airflow velocity using the PIV data-processing procedure described above. The experimental results

are shown in Figs. 10 and 11. The jet stream from the supply opening at the window-side near the driver's seat passed over the top of the back of the driver's seat, reaching part of the ceiling above the rear seat. The airflow velocity reached a maximum of 2.76 m/s in the region of the supply opening and began to decrease sharply from a point at approximately X = 600 mm. The air that had reached the ceiling of the model formed a large circulatory flow in the space between the driver's seat and the rear seat (Zone A) as it was interrupted by the back of the rear seat. Part of that air passed through Zone B and was exhausted from the exhaust opening. Figs. 12 and 13 show the airflow velocity distributions of the U and W components into which the jet stream was separated. The airflow velocity of the U component is approximately 2.5 times that of the W component.

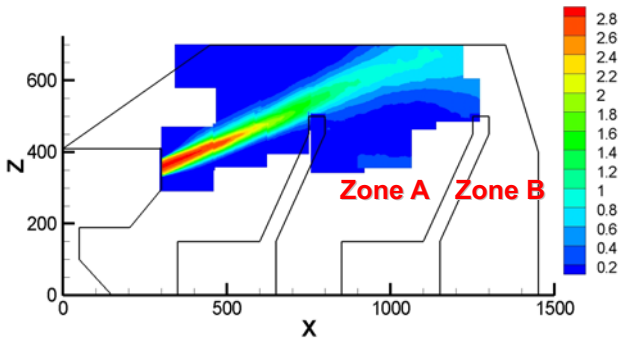

Fig. 10. Scalar profile of *UW* (graph unit: m/s)

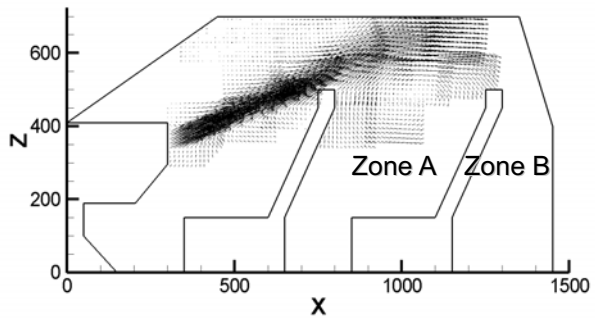

Fig. 11. Vector profile of *UW*

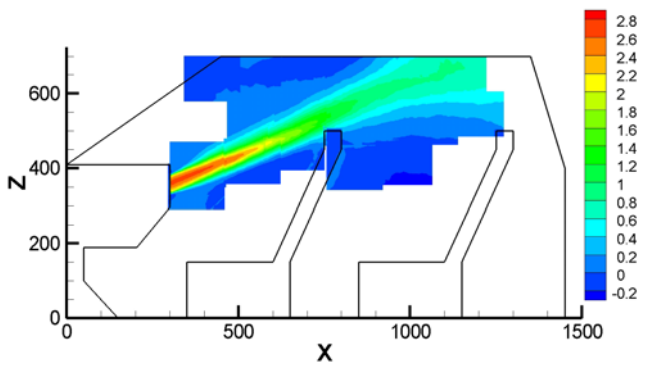

Fig. 12. Scalar profile of *U* (graph unit: m/s)

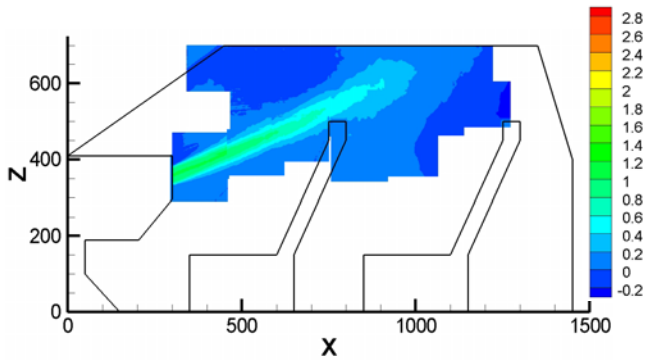

Fig. 13. Scalar profile of *W* (graph unit: m/s)

3) Distribution of Standard Deviation and Turbulence Intensity

The standard deviation (S.D.) of the instantaneous velocity relative to the average airflow velocity can be obtained by the following equation in *UW*:

$$S.D._i = \sqrt{\frac{\sum_{k=1}^{N} (\tilde{u}\tilde{w}_{i,k} - UW_i)^2}{N}} \tag{3}$$

Fig. 14 shows the standard deviation of *UW*. The standard deviation of the jet stream from the supply opening is less than 0.5m/s in the core zone up to the X = 550 mm point—about four times the opening diameter away from the supply opening (size: 50 mm × 60 mm). However, beyond the core zone (transient Zone), the standard deviation is 0.5m/s or more as mixing of the jet stream with the surrounding air is promoted. It can also be seen that the standard deviation of the lower portion of the jet stream is 1 to 1.5 times larger than that of the upper part of the jet stream.

Fig. 15 and Fig. 16 show the standard deviation of U and W respectively. The standard deviations of U and W are obtained by substituting $\tilde{u}\tilde{w}$ and UW in equation (3) with U and W components. The standard deviation of U turns out to be similar to that of UW. In the transient zone of the jet stream, however, U forms the sphere higher than 0.5 m/s more narrowly than UW. The maximum standard deviation of W in the core zone is 0.25 m/s, and that in the transient zone is 0.4 m/s, but the effect of this on the output of UW turned out to be very insignificant. It can thus be concluded that the air stream in a car air-condition is predominantly affected by the U element.

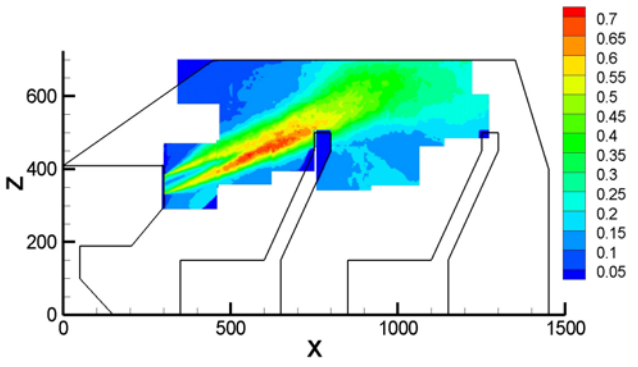

Fig. 14. S.D. distribution of UW (graph unit: m/s)

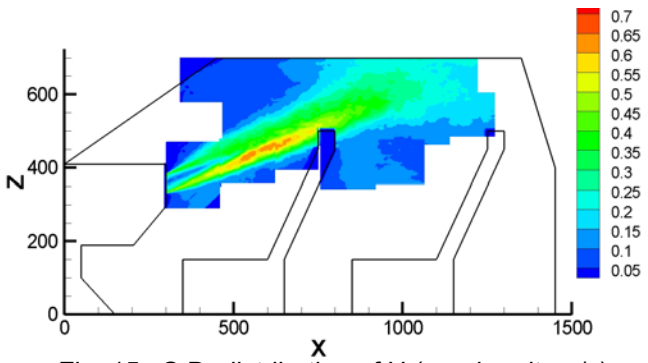

Fig. 15. S.D. distribution of U (graph unit: m/s)

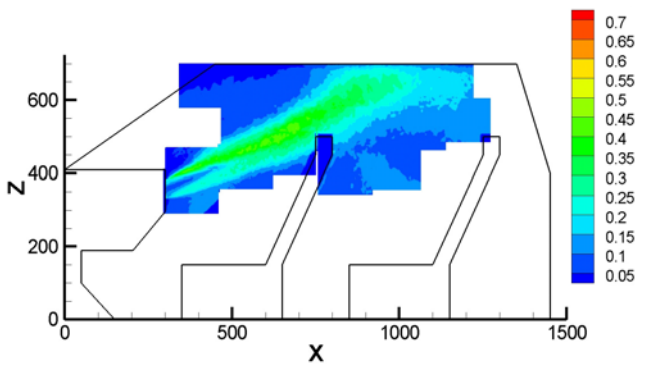

Fig. 16. S.D. distribution of W (graph unit: m/s)

The turbulence intensity (T.I.) of UW can be obtained from the following equation using the maximum airflow velocity of jet stream and the standard deviation (S.D.) calculated from Equation 3:

$$T.I._{\cdot i} = \frac{S.D._{\cdot i}}{UW_{\max}} \times 100 \tag{4}$$

Fig. 17 shows the turbulence intensity of UW. $UW_{\max}$ was 2.76 m/s, the previously measured maximum-supply air velocity. In the core zone of the jet stream, the turbulence intensity is around 15%. In the transient zone (Zone C), the maximum turbulence intensity is around 30%, which means that a driver's face is exposed to an airflow velocity of 2 m/s and to a turbulence intensity of 30%. If this is applied to the research result of Fanger et al. (1986, 1989), it is expected that if the temperature around the driver's seat is 296 K, more than 50% of all drivers will show dissatisfaction with the air stream. Therefore, when a car is air-conditioned, the jet stream should not be directed towards the face of the driver. On the other hand, as for the back seat (Zone D), a turbulence intensity of under 10% and an air velocity of under 0.2 m/s are formed. An air stream dissatisfaction rate of under 10% is therefore expected to be brought forth, according to the research of Fanger et al. That is, at the back seat, which is not directly affected by the jet stream, a calm environment is formed, which will lower the level of dissatisfaction of the passenger with the air stream.

Fig. 18 and Fig. 19 show the turbulence intensities of U and W, respectively. The turbulence intensities of U and W are obtained by substituting $\widetilde{u}\widetilde{w}$ and UW, $UW_{\max}$ in equations (3) and (4) with the elements of U and W, respectively. $U_{\max}$ (2.56 m/s) and $W_{\max}$ (1.05 m/s) are used in consideration of the measurement results. The turbulence intensity of U turns out to be similar to that of UW. On the other hand, W is found to have a turbulence intensity of 30~50% in the transient zone of the jet stream. This proves that the air stream inside a car is predominantly affected by the U component.

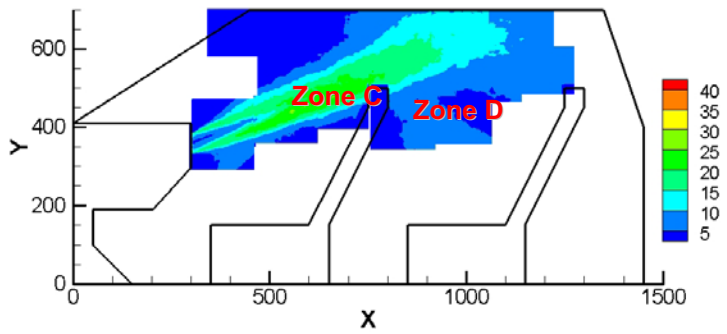

Fig. 17. T.I. distribution of UW (graph unit: %)

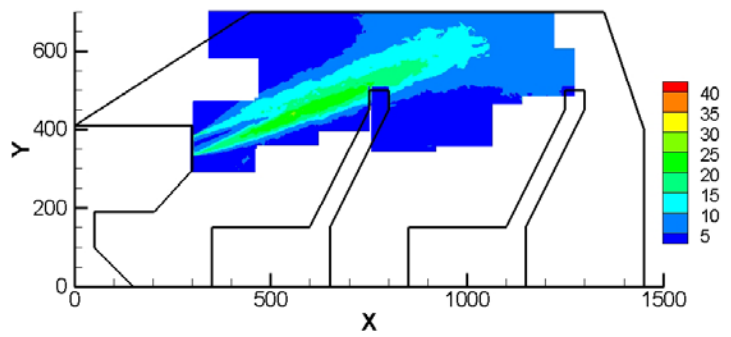

Fig. 18. T.I. distribution of U (graph unit: %)

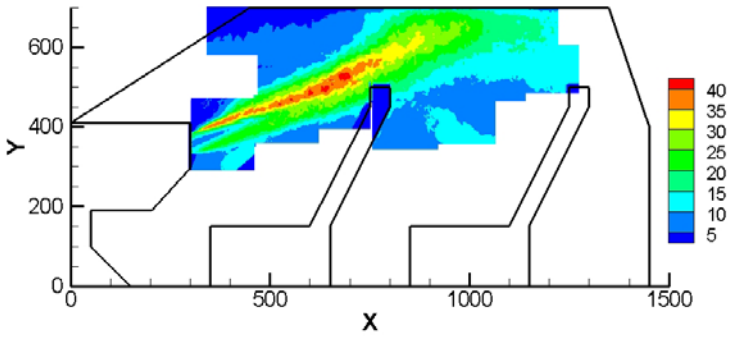

Fig. 19. T.I. distribution of W (graph unit: %)

4. Conclusion

In the present study, a ½ scale standard car model was created and a high precision PIV experiment was carried out using the model with the aim of providing data to examine the accuracy of CFD analysis.

Using a PIV system, the airflow characteristics in the model were measured, while the model interior was air-conditioned at a preset airflow rate (100 m^3/h).

At the average airflow velocity, the jet stream passed over the top of the back of the driver's seat, reaching the zone of the ceiling above the rear seat. The maximum airflow velocity reached 2.76 m/s in the region of the supply opening and began to decrease sharply in the 600-mm zone on the X-axis.

The standard deviation of *UW* was less than 0.5m/s in the core zone from the supply opening to X = 550 mm, approximately four times the diameter of the jet stream supply opening. Beyond the core zone (transient zone), however, the standard deviation was at least 0.5m/s as the mixing of the jet stream with the surrounding air was promoted.

In terms of the turbulence intensity of *UW*, the turbulence intensity of the jet stream in the

core zone was approximately 15%. In the transient zone, the maximum turbulence intensity was around 30%, which means that a driver's face is exposed to an airflow velocity of 2 m/s and to a turbulence intensity of 30%. This is that 50% of all drivers will show dissatisfaction with the air stream. Therefore, when a car is air-conditioned, the jet stream should not be directed towards the face of the driver.

References

Batterman, S., Jia, C.R., Hatzivasilis, G. and Godwin, C, Simultaneous measurement of ventilation using tracer gas techniques and VOC concentration in home, garages and vehicles, Journal of environmental monitoring, 8-2 (2006), 249-256

Dag Aronson, Zenitha Chroneer, Per Elofsson and Henrik Fellbom, Comparison Between CFD and PIV Measurements in a Passenger Compartment, SAE technical paper (2000)

Kataoka, T. and Fusada, Y., Evaluation of thermal environment in a vehicle compartment using a model of human thermal system, The Japan society of mechanical engineers, No. 628 (1998), 4261-4266

Kataoka, T. and Nakamura, Y., Prediction of thermal sensation based on simulation of temperature distribution in a vehicle cabin, Heat Transfer Asian Research, Vol.30 Issue3 (2001), 195-212

Installation & User's guide Book, 2004, Dantec

Fanger, P.O., Melikov, A.K., Hanzawa, H. and Ring, J., Turbulence and draft, ASHRAE Journal, 31-4 (1989), 18-25

Fanger, P.O. and Christensen, N.K., Perception of draft in ventilated space, Ergonomics, 29-2 (1986), 215-235

ASHRAE Fundamental Handbook, Chapter 8 Thermal Comfort (2001) ASHRAE

White FM, Fluid mechanics (2003) McGraw-Hill

Author Profile

Jeong-Hoon Yang: Yang received his M.Sc .(Eng) in Architecture Engineering in 2002 from the University of Tokyo. He received his Ph.D. in Architecture Engineering in 2005 also from the University of Tokyo. He worked at the Institute of Industrial Science, the University of Tokyo as a post-doctor in 2005. He has worked at the School of Architecture, Yeungnam University as an assistant professor since 2006. His research interests are Airflow Visualization, PIV, CFD, Ventilation Efficiency, and Thermal Comfort in architectural space.

Shinsuke Kato: For more than 20 years, Prof. Kato has managed the research on Building and Environmental Control Engineering at the Institute of Industrial Science, the University of Tokyo, since graduating from the University of Tokyo (Department of Engineering, Faculty of Architecture). He has been engaged in special research into the experimental study and the numerical simulation of turbulent airflow in rooms and around buildings.

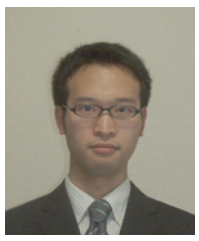

Hideaki Nagano: Nagano received his master's degree in Architecture Engineering in 2008 from the University of Tokyo. He is a Ph. D. student at the University of Tokyo. His research interests are human sensation for indoor environment, airflow and temperature distributions in rooms, and ventilation efficiency.